J. Fluid Mech. (1971), *vol.* 48, *part* 4, *pp.* 647–672
Printed in Great Britain

Contained non-homogeneous flow under gravity or how to stratify a fluid in the laboratory

By GÖSTA WALIN

Swedish Natural Science Research Council and
International Meteorological Institute in Stockholm, Sweden

(Received 9 February 1970 and in revised form 13 October 1970)

It is demonstrated that the basic stratification in a fluid region subject to thermal forcing may be predicted rather simply for a fairly wide class of boundary conditions. Explicit solutions are derived in certain cases. A useful experimental method for maintaining a stratified system with arbitrarily specified vertical variation of density emerges from the analysis. A preliminary laboratory experiment has demonstrated the efficiency of this method. The restrictions on the validity of the theory involve a limitation on the thermal forcing of the fluid, which may be expressed as an upper limit on the thermal conductance of the boundary of the region. Furthermore, the buoyancy frequency characterizing the solution must be sufficiently large to give rise to a boundary-layer-type flow pattern.

1. Introduction

The present paper tackles the problem of determining the density field in a closed region of general shape (figure 1), from the thermal and kinematic boundary conditions applied at the boundary of the region. We are concerned primarily with the steady-state fields, but the time-dependent problem is also discussed in order to determine the time scales involved. We limit our attention to situations in which the momentum balance is dominated by the buoyancy force, at least in the main part of the region.

Although much work has been devoted to the field of stratified flow (for example, see Yih 1965), almost all of it has concentrated on the theory of perturbations on a prescribed stratification, while the problem of determining the basic stratification has been given little or no attention (as an example, Yih's book contains no reference at all to this problem). There are, however, a few exceptions. Gill (1966) with approximate boundary-layer methods studied the density and flow fields in a rectangular region with specified temperature on the vertical walls, and McIntyre (1968) studied a similar problem in a rotating frame. A rotation dominated problem involving an unknown basic density field was also studied by Barcilon & Pedlosky (1967) in a rather different parameter régime in which the centrifugal force was the important ingredient.

In their analyses, both Gill and McIntyre were forced to make some *ad hoc* approximations. Part of their difficulty is attributable to the choice of perfectly conducting boundaries. This paper shows that if we do not insist on these, but

drive the fluid with boundaries of finite conductance, the problem becomes a good deal more tractable. At the same time it becomes more realistic, and leads to a powerful laboratory technique for producing any specified stratification.

There are two types of situations in which the temperature distribution in a fluid system influenced by gravitation may be obtained in an obvious way. First we have the case when the heat balance is dominated by diffusion, the simplest case being a fluid region between a warm top and cold bottom, the top and bottom coinciding with geopotential surfaces. Secondly we have the case when the temperature is prescribed on all boundaries of the region but in such a way that boundary points on the same geopotential surface have the same temperature. In this case diffusion may be arbitrarily weak (although not absent), and actually if it is 'sufficiently' weak the fluid temperature simply equals the boundary temperature at the same geopotential surface. Some aspects of this problem (although formulated as a perturbation problem) have been discussed by Veronis (1967*a*, *b*).

Obviously there exists a wide class of boundary conditions which give rise to a temperature distribution dominated by a stable stratification, although this stratification is not predictable as trivially as in the above examples. In the present paper, part of this prediction problem is tackled.

Outline of approach and main results

In § 2 we derive the lowest-order equations governing the interior of the fluid region, under the constraint that the density variation is sufficiently large for the momentum balance to be dominated by the buoyancy force. This basic constraint may also be expressed as a requirement that the buoyancy frequency is much larger than other frequencies characterizing the system. The drastic (though not unexpected) consequence of this assumption is that, in the interior, the density as well as the vertical velocity is forced to be a function of vertical co-ordinate z and time t only.

The degenerate behaviour of the interior requires the existence of boundary layers, which are analyzed in § 3. From this analysis emerges a general condition for the boundary-layer equations to linearize (and reduce to the buoyancy-layer equations). Thus we must require that the maximum density variation across the boundary layer should be small when compared with the density variation throughout the fluid. It is shown that this in general means that the boundary of the region has to be a *sufficiently poor conductor*, but other possible cases exist, such as the one treated by Veronis (1967*a*, *b*).

After establishing validity of the linear buoyancy-layer equations, we may express the boundary-layer transport in terms of the unknown interior fields and the boundary conditions. This relation is then used in § 4 to close the interior problem. The result is a linear differential equation in z and t from which the interior density field $\rho^I(z, t)$ may be determined.

At the end of § 4 we discuss briefly the transient behaviour of $\rho^I(z, t)$ and point out the very important feature that the adjustment time to steady state may to some extent be controlled in an experiment, for example substantially reduced below the so-called diffusion time.

In §5 we apply the general results of §4 to a cylindrical region with axis perpendicular to the gravitational force $g\mathbf{k}$, and in §6 we consider a region with rectangular cross-section. The results of §6 have been checked with a preliminary experiment reported in §7. In §8 finally, we summarize the restrictions on the analysis and discuss its range of validity.

Carefully notice that in §2 and most of §3, non-dimensional variables are used in the process of finding the lowest-order dynamical balances, while at the end of §3 and in §§4–8, we use dimensional variables in order to have closer contact with the physical characteristics of the system.

2. The strongly stratified interior

Within the Boussinesq approximation the equations governing a non-homogeneous fluid under gravity may be written

$$\rho_m d\mathbf{v}/dt = -\nabla p + \rho g\mathbf{k} + \rho_m \nu \nabla^2 \mathbf{v}, \tag{2.1a}$$

$$d\rho/dt = \kappa \nabla^2 \rho, \tag{2.1b}$$

$$\nabla . \mathbf{v} = 0, \tag{2.1c}$$

where $\mathbf{v}$ is the velocity vector with components (U, V, W) and $\mathbf{k}$ the vector $(0, 0, -1)$ in the Cartesian co-ordinate system (x, y, z), ρ and p are deviations in density and pressure from the mean density ρ_m and the associated hydrostatic pressure $(-\rho_m g z + \text{const.})$, ν and κ are the diffusivities of momentum and density (i.e. temperature), and g is the gravitational acceleration. The fluid is bounded by a rigid surface S on which we require

$$\left.\begin{aligned} \mathbf{v} &= 0 && (2.2a)\\ \mathbf{n} . \nabla \rho &= s(\rho - \hat{\rho}) && (2.2b) \end{aligned}\right\} \text{ on } S,$$

where $\mathbf{n}$ is the inward unit normal to the boundary, while s and $\hat{\rho}$ are known functions of time and position on the boundary.

Equations (2.1) and (2.2) will now be non-dimensionalized with the following transformations:

$$(x, y, z) = L(x', y', z'), \tag{2.3a}$$

$$t = \tau t', \tag{2.3b}$$

$$(U, V, W) = U_0(U', V', W'), \tag{2.3c}$$

$$p = Pp', \tag{2.3d}$$

$$\rho = Q\rho'. \tag{2.3e}$$

We assume that the scale of density variation Q is also representative for the forcing field $\hat{\rho}$, i.e.

$$Q \sim \hat{\rho}. \tag{2.4}$$

We also assume that L is known, and representative for the size of the container, while P, U_0 and τ in general are unknown *a priori*. Furthermore, U_0 will be chosen as representative for the largest velocity in the fluid. (This will mean in general that $|\mathbf{v}| \ll U_0$ in the interior, since the largest velocity is found in the boundary layer; see §3.2.)

Dropping the primes, we obtain

$$\delta_N R_N \frac{\partial \mathbf{v}}{\partial t} + R_N^2 \mathbf{v}.\nabla\mathbf{v} = -\frac{P}{QgL}\nabla p + \rho\mathbf{k} + R_N E_N \nabla^2 \mathbf{v}, \tag{2.5a}$$

$$\delta_N \partial\rho/\partial t + R_N \mathbf{v}.\nabla\rho = \sigma^{-1} E_N \nabla^2 \rho, \tag{2.5b}$$

$$\nabla.\mathbf{v} = 0, \tag{2.5c}$$

with boundary conditions

$$\left.\begin{aligned} \mathbf{v} &= 0 \\ \mathbf{n}.\nabla\rho &= sL(\rho - \hat{\rho}Q^{-1}) \end{aligned}\right\} \text{ on } S, \tag{2.5d,e}$$

where

$$\delta_N = (\tau N)^{-1} \tag{2.6a}$$

$$R_N = U_0 L^{-1} N^{-1}, \tag{2.6b}$$

$$E_N = \nu L^{-2} N^{-1}, \tag{2.6c}$$

$$\sigma = \nu\kappa^{-1}. \tag{2.6d}$$

The parameter N may be called characteristic buoyancy frequency and is defined by

$$N^2 = Qg/\rho_m L. \tag{2.6e}$$

We are interested here in the stratification-dominated régime characterized by

$$\delta = \max(\delta_N, R_N, E_N) \ll 1, \tag{2.7a}$$

$$\sigma \sim 1. \tag{2.7b}$$

Under this constraint the momentum equation (2.5a) becomes hydrostatic to lowest order in δ,

$$(-P/QgL)\nabla p + \rho\mathbf{k} = 0. \tag{2.8a}$$

For consistency we require

$$P = QgL. \tag{2.8b}$$

Taking the curl of (2.8a) we obtain

$$\nabla\rho \times \mathbf{k} = 0. \tag{2.8c}$$

If we limit our attention to regions such that each horizontal cross-section is a connected surface, (2.8c) is equivalent to

$$\rho = \rho(z, t). \tag{2.9a}$$

When (2.9a) is introduced into the diffusion equation (2.5b), we obtain

$$\delta_N \frac{\partial}{\partial t}\rho(z,t) + R_N W \frac{\partial}{\partial z}\rho(z,t) = \sigma^{-1} E_N \frac{\partial^2}{\partial z^2}\rho(z,t), \tag{2.9b}$$

which requires

$$W = W(z, t). \tag{2.9c}$$

Equations (2.9) together with continuity are the lowest-order equations governing a fluid system satisfying conditions (2.7). It seems convenient to call such a system 'strongly stratified'. This definition bears a close correspondence to the concept 'rapidly rotating' and its mathematical expression in the Taylor–Proudman theorem.

Obviously, velocity and density fields constrained by (2.9) can only satisfy very special boundary conditions. We expect accordingly that our scaling assumptions will break down somewhere in the region. Assuming this breakdown to occur close to the boundaries, we will now try a boundary-layer approach to the problem.

3. The boundary layer

Let us assume that the solution consists of two parts according to

$$\phi = \phi^I + \phi^B, \tag{3.1a}$$

where ϕ represents any one of the dependent variables. Furthermore, ϕ^I is assumed to satisfy equations (2.5*a–c*) and to have the scale properties postulated when deriving equations (2.9). Thus by definition (2.9) are the lowest-order equations for ϕ^I. ϕ^B, on the other hand, is assumed to be negligibly small everywhere except in a thin layer close to the boundary. While varying with the interior scale L along the boundary, ϕ^B is thus assumed to vary much faster in a direction perpendicular to the boundary. Suppose provisionally that this variation is characterized by a single scale ϵL where $\epsilon \ll 1$.

If equations (2.5*a–c*) are written symbolically as

$$\mathscr{P}(\phi) = 0, \tag{3.1b}$$

we have by definition $$\mathscr{P}(\phi^I) = \mathscr{P}(\phi^I + \phi^B) = 0, \tag{3.1c}$$

and consequently $$\mathscr{P}(\phi^I + \phi^B) - \mathscr{P}(\phi^I) = 0. \tag{3.1d}$$

Equation (3.1*d*) will now be written in a local unstretched Cartesian co-ordinate system (ξ, η, ζ) attached to the boundary and oriented in such a way that the ζ axis coincides with the local inward normal to the boundary. For the moment we assume that the ζ axis is not vertical, that the η axis is perpendicular to the gravitational force $g\mathbf{k}$, and that the ξ axis has a positive upward component (see figure 1). The co-ordinates are scaled by L as in (2.3*a*).

We obtain in non-dimensional form

$$\delta_N R_N \frac{\partial u^B}{\partial t} + R_N^2 \mathscr{N}_\xi = -\frac{\partial p^B}{\partial \xi} + k_\xi \rho^B + R_N E_N \nabla^2 u^B, \tag{3.2a}$$

$$\delta_N R_N \frac{\partial v^B}{\partial t} + R_N^2 \mathscr{N}_\eta = -\frac{\partial p^B}{\partial \eta} + R_N E_N \nabla^2 v^B, \tag{3.2b}$$

$$\delta_N R_N \frac{\partial w^B}{\partial t} + R_N^2 \mathscr{N}_\zeta = -\frac{\partial p^B}{\partial \zeta} + k_\zeta \rho^B + R_N E_N \nabla^2 w^B, \tag{3.2c}$$

$$\delta_N \frac{\partial \rho^B}{\partial t} + R_N \mathscr{N}_\rho = \sigma^{-1} E_n \nabla^2 \rho^B, \tag{3.2d}$$

$$\frac{\partial u^B}{\partial \xi} + \frac{\partial v^B}{\partial \eta} + \frac{\partial w^B}{\partial \zeta} = 0, \tag{3.2e}$$

where $(k_\xi, 0, k_\zeta)$ is the local representation of the vector $\mathbf{k}$ and

$$(u, v, w) = (u^I, v^I, w^I) + (u^B, v^B, w^B)$$

represents the velocity $\mathbf{v}$ in the local co-ordinate system (ξ, η, ζ). The interaction terms in (3.2) are defined by

$$\mathscr{N}_\xi = \mathbf{v}^B.\nabla u^B + \mathbf{v}^B.\nabla u^I + \mathbf{v}^I.\nabla u^B, \tag{3.2f}$$

$$\mathscr{N}_\eta = \mathbf{v}^B.\nabla v^B + \mathbf{v}^B.\nabla v^I + \mathbf{v}^I.\nabla v^B, \tag{3.2g}$$

$$\mathscr{N}_\zeta = \mathbf{v}^B.\nabla w^B + \mathbf{v}^B.\nabla w^I + \mathbf{v}^I.\nabla w^B, \tag{3.2h}$$

$$\mathscr{N}_\rho = \mathbf{v}^B.\nabla \rho^B + \mathbf{v}^B.\nabla \rho^I + \mathbf{v}^I.\nabla \rho^B. \tag{3.2i}$$

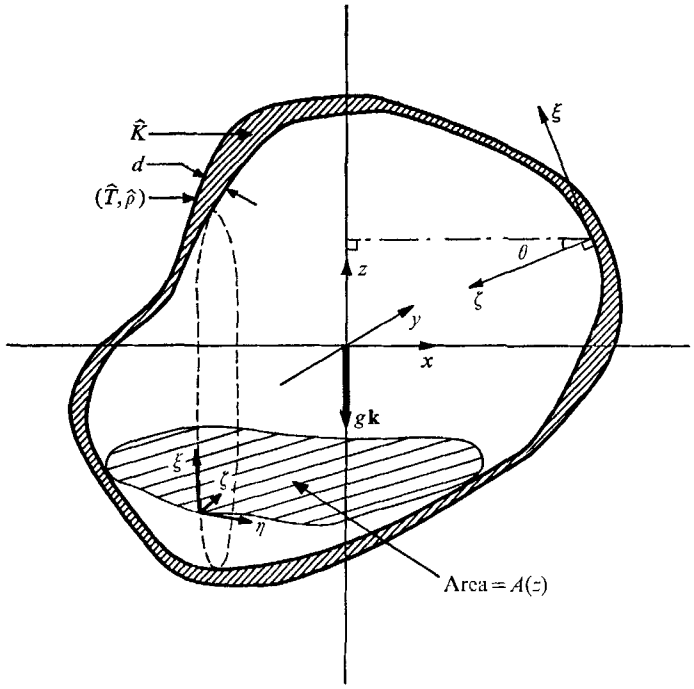

FIGURE 1. Illustration of the geometry of the general problem dealt with in §§2–4. The local co-ordinate system (ξ, η, ζ) is so defined that the ζ axis coincides with the inward normal to the boundary, the η axis is perpendicular to the gravity force $g\mathbf{k}$, and the ξ axis has a positive upward component. The imposed outside temperature $\hat{T}$ (corresponding to fluid density $\hat{\rho}$), the wall thickness d as well as the conductivity $\hat{K}$ is allowed to vary along the boundary. It should be remembered, however, that the correspondence between the illustrated arrangement and the mathematical problem is good only when $d \ll L$.

The boundary conditions (2.5d, e) are required to be satisfied by the complete solution $\phi^I + \phi^B$. We have for the local form of the boundary condition

$$\left.\begin{aligned} &\mathbf{v}^I + \mathbf{v}^B = 0 && (3.3a)\\ &\frac{\partial \rho^I}{\partial \zeta} + \frac{\partial \rho^B}{\partial \zeta} = sL(\rho^I + \rho^B - \hat{\rho}Q^{-1}) && (3.3b) \end{aligned}\right\} \quad \text{at} \quad (\xi, \eta, \zeta) = 0.$$

Our aim now is to solve (3.2) for ϕ^B, subject to (3.3), considering ϕ^I as known. We can then express ϕ^B in terms of ϕ^I, making it possible to eliminate ϕ^B from the boundary condition (3.3), which would close the problem for ϕ^I.

To obtain a consistent lowest-order set of equations from (3.2) and (3.3) we shall make use of conditions (2.4) and (2.7) together with the postulated properties of ϕ^B. In the neighbourhood of the boundary point $(\xi, \eta, \zeta) = 0$ these may be expressed as

$$\frac{\partial}{\partial \xi}\phi^B \sim \epsilon^{-1}\phi^B, \tag{3.4a}$$

$$\frac{\partial}{\partial \xi}\phi^B \sim \frac{\partial}{\partial \eta}\phi^B \sim \phi^B, \tag{3.4b}$$

where

$$\epsilon \ll 1. \tag{3.4c}$$

3.1. *The restriction on the thermal boundary condition*

However, an essential difficulty is associated with the non-linear term $\mathscr{N}_\rho$ in the heat equation (3.2*d*). The usual way to avoid this difficulty is to limit the study to small deviations from a given stratification, thereby giving up any attempt to predict the main density field. Technically this means that the linearization and consequent simplification is performed before the splitting of the dependent variables into interior and boundary-layer parts. In the present approach we simplify the equations for ϕ^I and ϕ^B separately, starting with the complete non-linear equations (3.1*c*) and (3.1*d*) respectively. As we shall find, this can be done without giving up the attempt to predict the main density field ρ^I. The lowest-order equations for ϕ^I have already been derived (2.9); what remains is the simplification of (3.1*d*), i.e. of (3.2).

It turns out that if

$$\rho^B \ll 1, \tag{3.5}$$

$\mathscr{N}_\rho$ simplifies to

$$\mathscr{N}_\rho = \mathbf{v}^B . \nabla \rho^I. \tag{3.6}$$

This form of $\mathscr{N}_\rho$, though still expressing the interaction between two unknown fields, is linear with respect to ϕ^B, which is sufficient for this part of the problem to be tractable. Equation (3.5) will therefore be adopted as an additional restriction on our analysis. Observe, however, that justification of (3.6) also requires some knowledge of the relative order of magnitude of the velocity components as given by (3.11) below.

Before making use of (3.5), we will examine the restrictions that have to be imposed on the boundary condition in order that (3.5) be satisfied. The boundary condition on ρ (3.3*b*) may be written

$$\left(\frac{\partial}{\partial \xi} - sL\right)\rho^B = sL(\rho^I - \hat{\rho}Q^{-1}) - \frac{\partial}{\partial \xi}\rho^I \quad \text{at} \quad (\xi, \eta, \zeta) = 0. \tag{3.7}$$

From (3.4) and our previous assumption that $\hat{\rho}Q^{-1} \sim \rho^I \sim 1$, we obtain the following estimates

$$\frac{\partial}{\partial \xi}\rho^B \sim \epsilon^{-1}\rho^B, \quad \rho^I - \hat{\rho}Q^{-1} \sim 1, \quad \frac{\partial}{\partial \xi}\rho^I \lesssim 1,$$

which we introduce in (3.7), obtaining

$$\rho^B . \max(\epsilon^{-1}, sL) \lesssim \max(sL, 1). \tag{3.8}$$

Remembering that $\epsilon \ll 1$ it follows that $\rho^B \ll 1$ if

$$sL \ll \epsilon^{-1}, \tag{3.9}$$

which is the required restriction on the thermal boundary condition.

In order to understand the physical meaning of (3.9), we may think of the boundary condition (3.3*b*) as realized by a wall of thickness d and conductivity $\hat{K}$, outside which the temperature is held at the value $\hat{T}$ corresponding to fluid density $\hat{\rho}$ (see figure 1). If d is small enough compared with the dimensions of the region, so that the tangential heat flux in the wall may be neglected, we have approximately

$$s = \hat{K}/Kd, \tag{3.10a}$$

where K is the thermal conductivity of the working fluid. Thus (3.9) may be written as

$$d^* = dK/\hat{K} \gg \epsilon L. \tag{3.10b}$$

Numerical values of the wall 'thermal thickness' d^* and the boundary-layer thickness ϵL are given in table 1 for some cases typical for laboratory application.

Fluid		Water	Alcohol	Mercury
Boundary-layer thickness $\epsilon L = (\kappa\nu/N)^{\frac{1}{4}}$ (cm)		0·11	0·073	0·16
'Thermal thickness' of boundary made of various materials $d^* = s^{-1} = d.K/\hat{K}$ (cm)	Plexiglass	3·2	0·11	65
	Glass	0·62	0·20	11·7
	Steel	0·010	0·0035	0·18
	Copper	0·0015	0·0005	0·028

TABLE 1. Typical values of boundary-layer thickness and 'thermal thickness' d^* of the boundary for various combinations of fluids and wall materials. Cases when $\epsilon L < d^*$ (i.e. $sL < E_N^{-\frac{1}{2}}$) are enclosed by a frame. The buoyancy frequency has been based on a temperature gradient of about 0·5 °C/cm, and the wall thickness d was chosen to be 1 cm. K and $\hat{K}$ are the thermal conductivities (e.g. measured in w/m.°C) of fluid and wall material respectively

3.2. *The buoyancy layer*

Before proceeding to the derivation of the lowest-order boundary-layer equations, we now have to settle the definition of $R_N \equiv U_0 N^{-1} L^{-1}$. Anticipating that the largest velocity in the fluid is the boundary-layer component represented by u^B, we choose U_0 to be representative of this velocity component. Thus we have

$$u^B \sim 1, \tag{3.11a}$$

and

$$(u^I, v^I, w^I) \lesssim 1. \tag{3.11b}$$

Furthermore, the continuity equation (3.2*e*) and the scale properties (3.4) imply

$$w^B \lesssim \epsilon, \tag{3.11c}$$

which in view of the boundary condition (3.3*a*) and the scale property of w^I means that

$$w^I \lesssim \epsilon \tag{3.11d}$$

at least in the boundary-layer region. From (3.11*a–d*), the scale properties (3.4), and the previous assumptions $\rho^B \ll 1$ and $\rho^I \sim 1$, it follows now that to lowest order $\mathscr{N}_\rho$ may be written

$$\mathscr{N}_\rho = u^B \frac{\partial \rho^I}{\partial \xi} + v^B \frac{\partial \rho^I}{\partial \eta}. \tag{3.11e}$$

It is essential that $\partial\rho^I/\partial\xi \sim 1$ for (3.11*e*) to be valid. This, however, follows from $\partial\rho^I/\partial z \sim 1$ (see §2), when the ζ axis is not vertical as we have assumed.

Imposing the additional restriction

$$\delta_N \ll E_N \epsilon^{-2}, \tag{3.11f}$$

the first term in the heat equation (3.2*d*) becomes negligibly small compared with the diffusion term. (In view of the result $\epsilon \sim E_N^{\frac{1}{2}}$ found below, (3.11*f*) will be implied by the already imposed condition on δ_N, (2.7).)

Utilizing the boundary-layer property of ρ^B in order to simplify the Laplacian, we thus obtain the lowest-order approximation for (3.2*d*)

$$R_N\left(u^B\frac{\partial\rho^I}{\partial\xi}+v^B\frac{\partial\rho^I}{\partial\eta}\right) = -\sigma^{-1}E_N\frac{\partial^2\rho^B}{\partial\zeta^2}. \tag{3.12a}$$

We now apply conditions (2.7), the scale properties of ϕ^I as well as ϕ^B, and the assumption that the dissipative processes enter the basic balance, to the remaining boundary-layer equations (3.2). To lowest order we obtain

$$0 = -\frac{\partial p^B}{\partial\xi}+k_\xi\rho^B+R_N E_N\frac{\partial^2 u^B}{\partial\zeta^2}, \tag{3.12b}$$

$$0 = -\frac{\partial p^B}{\partial\eta}+R_N E_N\frac{\partial^2 v^B}{\partial\zeta^2}, \tag{3.12c}$$

$$0 = -\frac{\partial p^B}{\partial\zeta}, \tag{3.12d}$$

$$\frac{\partial u^B}{\partial\xi}+\frac{\partial v^B}{\partial\eta}+\frac{\partial w^B}{\partial\zeta} = 0. \tag{3.12e}$$

Equations (3.12) become internally consistent if

$$\epsilon \sim E_N^{\frac{1}{2}}, \tag{3.13a}$$

$$\rho^B \sim R_N, \tag{3.13b}$$

$$p^B \lesssim R_N. \tag{3.13c}$$

Combining (3.13) with our previous estimate of ρ^B (3.8) and condition (3.9), we obtain

$$\rho^B \sim R_N \lesssim E_N^{\frac{1}{2}}\max(sL, 1). \tag{3.14}$$

Equations (3.12) may be further simplified by taking into account the definition that ϕ^B is non-zero only in the boundary layer

$$\lim_{\epsilon^{-1}\zeta\to\infty}\phi^B = 0, \tag{3.15}$$

and the lowest-order properties of ϕ^I expressed by equation (2.9), in particular the fact that $\partial\rho^I/\partial\eta = 0$. We obtain in *dimensional* form

$$\kappa\frac{\partial^2\rho^B}{\partial\zeta^2}-\frac{\partial\rho^I}{\partial\xi}u^B = 0, \tag{3.16a}$$

$$k_\xi g\rho^B+\nu\rho_m\frac{\partial^2 u^B}{\partial\zeta^2} = 0, \tag{3.16b}$$

$$\frac{\partial u^B}{\partial\xi}+\frac{\partial w^B}{\partial\zeta} = 0, \tag{3.16c}$$

$$v^B = p^B = 0. \tag{3.16d}$$

Equations (3.16a, b) represent a closed system of ordinary differential equations for u^B and ρ^B. Together with the dimensional form of the boundary condition (3.3), this system may be solved in terms of u^I, ρ^I, and the local values of s and $\hat{\rho}$. Note that, in consistency with the boundary-layer approximation, $\partial\rho^I/\partial\xi$ should be considered to be independent of ζ, and replaced by $(\partial\rho^I/\partial\xi)_{\zeta=0}$, while integrating the boundary-layer equations (3.16).

Equations (3.16) are equivalent to the 'buoyancy-layer' equations derived by Veronis (1967a), although they are derived here under substantially more general conditions.

Equations (3.16a, b) have solutions of the (dimensional) form

$$u^B = A\exp(-\tilde{\zeta})\begin{Bmatrix}\sin\tilde{\zeta}\\ \cos\tilde{\zeta}\end{Bmatrix}, \tag{3.17a}$$

$$\rho^B = B\exp(-\tilde{\zeta})\begin{Bmatrix}\cos\tilde{\zeta}\\ -\sin\tilde{\zeta}\end{Bmatrix}, \tag{3.17b}$$

where

$$\zeta/\tilde{\zeta} = 2^{\frac{1}{2}}\left|\left(\frac{\partial\rho^I}{\partial\xi}\frac{gk_\xi}{\kappa\nu\rho_m}\right)^{-\frac{1}{4}}\right| \sim E_N^{\frac{1}{2}}.L, \tag{3.17c}$$

$$B/A = \operatorname{sgn} k_\xi\left|\left(\frac{\partial\rho^I}{\partial\xi}.\frac{\nu\rho_m}{\kappa k_\xi g}\right)^{\frac{1}{2}}\right|. \tag{3.17d}$$

These solutions have the postulated decay property (3.15) and the scale property (3.4a) except at singular points where $k_\xi\partial\rho^I/\partial\xi$ vanishes. The problem connected with these points is very similar to the problem in rapidly rotating fluids, where the Ekman layer becomes (formally) infinitely thick on vertical boundaries. By analogy we can expect these singularities to have only a passive, local significance (e.g. see Stewartson 1966). Here we restrict ourselves to confirming this in the particular but typical examples discussed in §§5 and 6. The unknown constants in (3.17) may be determined, making use of the dimensional form of the boundary condition (3.3).

Having now established the existence of an appropriate boundary-layer solution, its explicit form will not be needed any more, since in the next section it will turn out that we can use a more direct approach to the closure of our basic 'interior problem'.

4. The ρ^I equation

Our next task is to derive closed equations for the interior fields, making use of both the lowest-order properties of ϕ^I and ϕ^B (derived in §§2 and 3) and the boundary conditions (3.3). In this and following sections we will use only *dimensional* variables, without change of notation. The simultaneous use of two different co-ordinate systems may be a cause of confusion. Observe, therefore, the notation (U, V, W) for the velocity in the system (x, y, z) oriented with the z axis parallel to the gravitational force and (u, v, w) for the velocity in the (ξ, η, ζ) system. In dimensional form our lowest-order equations become:

interior part of the solution

$$\rho^I = \rho^I(z, t), \tag{4.1a}$$

$$W^I = W^I(z, t), \tag{4.1b}$$

$$\frac{\partial \rho^I}{\partial t} + W^I \frac{\partial \rho^I}{\partial z} = \kappa \frac{\partial^2 \rho^I}{\partial z^2}; \tag{4.1c}$$

boundary-layer part

$$k_\xi g \rho^B + \nu \rho_m \frac{\partial^2 u^B}{\partial \zeta^2} = 0, \tag{4.2a}$$

$$\kappa \frac{\partial^2 \rho^B}{\partial \zeta^2} - \left(\frac{\partial \rho^I}{\partial \xi}\right)_{\zeta=0} u^B = 0, \tag{4.2b}$$

together with the boundary condition for the complete solution

$$\left.\begin{aligned} \mathbf{v}^I + \mathbf{v}^B &= 0 \qquad (4.3a)\\ \frac{\partial \rho^I}{\partial \zeta} + \frac{\partial \rho^B}{\partial \zeta} &= s(\rho^I + \rho^B - \hat{\rho}) \qquad (4.3b) \end{aligned}\right\} \quad \text{at} \quad (\xi, \eta, \zeta) = 0.$$

From (4.1) and (4.2) the continuity equation has been omitted. Instead we add a continuity requirement of the form

$$M^T(z,t) = 0, \tag{4.4}$$

where M^T represents the total volume flow through a horizontal surface at height z.

M^T is composed of two parts according to

$$M^T = A(z)\, W^I(z,t) + M^B(z,t), \tag{4.5}$$

where $A(z)$ is the horizontal surface area occupied by the fluid region at height z, and M^B is the total transport carried by the boundary layer through the same surface. M^B may be expressed in terms of u^B according to

$$M^B = \oint dl . \int_0^\infty u^B d\zeta = \oint m\, dl, \tag{4.6}$$

where $\oint dl$ represents a line integral around the horizontal surface with area $A(z)$.

Integrating equation (4.2*b*) with respect to ζ, utilizing (3.15), we obtain

$$m = -\kappa \left(\frac{\partial \rho^I}{\partial \xi}\right)^{-1}_{\zeta=0} \left(\frac{\partial \rho^B}{\partial \zeta}\right)_{\zeta=0}. \tag{4.7}$$

In view of (3.4) and (3.5) the thermal boundary condition takes on the approximate form

$$\frac{\partial \rho^I}{\partial \zeta} + \frac{\partial \rho^B}{\partial \zeta} = s(\rho^I - \hat{\rho}) \quad \text{at} \quad \zeta = 0. \tag{4.8}$$

Introducing (4.8) in (4.7), we obtain

$$m = -\left[\left(\frac{\partial \rho^I}{\partial \xi}\right)^{-1} \left(s(\rho^I - \hat{\rho}) - \frac{\partial \rho^I}{\partial \zeta}\right)\right]_{\zeta=0}. \tag{4.9}$$

Since ρ^I depends only on (z,t), $\partial \rho^I/\partial \xi$ and $\partial \rho^I/\partial \zeta$ are completely determined by $\partial \rho^I/\partial z$ and the slope of the boundary. If we define an angle θ, $-\frac{1}{2}\pi \leqslant \theta \leqslant \frac{1}{2}\pi$, such

that $\theta+\frac{1}{2}\pi$ is the angle between the inward normal to the boundary and the positive z axis (see figure 1), we have

$$\frac{\partial\rho^I}{\partial\xi}=\cos\theta\frac{\partial\rho^I}{\partial z}, \tag{4.10a}$$

$$\frac{\partial\rho^I}{\partial\zeta}=-\sin\theta\frac{\partial\rho^I}{\partial z}. \tag{4.10b}$$

When (4.9) and (4.10) are introduced into (4.6) we obtain

$$M^B=\oint-\kappa\left(\frac{\partial\rho^I}{\partial z}\right)^{-1}\left(\tan\theta\frac{\partial\rho^I}{\partial z}+\frac{s(\rho^I-\hat{\rho})}{\cos\theta}\right)dl. \tag{4.11}$$

Observe that ρ^I and $\partial\rho^I/\partial z$ are constant along the path of integration and may be moved outside the integral sign.

Using the continuity requirement (4.4), we can now express the vertical velocity in the diffusion equation (4.1c) in terms of ρ^I and thereby produce a single equation for ρ^I alone. From (4.4), (4.5) and (4.11), we obtain

$$W^I(z,t)=\frac{\kappa}{A}\left(\frac{\partial\rho^I}{\partial z}\right)^{-1}\left(-\frac{dA}{dz}\frac{\partial\rho^I}{\partial z}+\oint\frac{s(\rho^I-\hat{\rho})}{\cos\theta}dl\right), \tag{4.12}$$

where we have made use of the identity

$$\oint\tan\theta\,dl=-\frac{dA}{dz}. \tag{4.13}$$

When (4.12) is introduced in (4.1c) we obtain the required equation for ρ^I

$$\frac{\partial\rho^I}{\partial t}-\kappa\frac{\partial^2\rho^I}{\partial z^2}-\frac{\kappa}{A}\frac{dA}{dz}\frac{\partial\rho^I}{\partial z}+\frac{\kappa}{A}\oint\frac{s(\rho^I-\hat{\rho})}{\cos\theta}dl=0, \tag{4.14a}$$

which may also be written

$$\frac{\partial\rho^I}{\partial t}-\frac{\kappa}{A}\frac{\partial}{\partial z}\left(A\frac{\partial\rho^I}{\partial z}\right)+B(z)\rho^I=C(z), \tag{4.14b}$$

where

$$B(z)\equiv\frac{\kappa}{A}\oint\frac{s\,dl}{\cos\theta},\quad C(z)\equiv\frac{\kappa}{A}\oint\frac{s\hat{\rho}\,dl}{\cos\theta}. \tag{4.14c}$$

It is remarkable that because of the appearance of the factor $(\partial\rho^I/\partial z)^{-1}$ in the expression (4.12) for W^I, elimination of W^I has resulted in a *linear* equation for ρ^I.

The foregoing ideas will be illustrated by means of two specific examples in §§5 and 6. Here we will only point out a few important properties of equations (4.14).

4.1. *The case* $1\ll sL\ll E_N^{\frac{1}{2}}$

Estimating the terms in (4.14b) we find that when $sL\gg1$, the *steady* solution degenerates to

$$\rho^I=\oint\frac{s\hat{\rho}\,dl}{\cos\theta}\Big/\oint\frac{s\,dl}{\cos\theta}. \tag{4.15}$$

By comparison with (4.11) we find that with the same degree of approximation this is equivalent to

$$M^B=0. \tag{4.16}$$

Thus when sL is large, the net boundary-layer flux through a horizontal surface must vanish. Note that ρ^I *is thereby determined for each level individually*. Complications associated with this degeneracy are discussed in §6.

4.2. *Adjustment time*

The time τ required for the density field to approach steady state may be determined by assuming balance between $\partial\rho^I/\partial t$ and the largest of the other terms in (4.14*b*). We obtain

$$\tau \sim \min\left(\frac{L^2}{\kappa}, \frac{L^2}{\kappa}\frac{1}{sL}\right). \tag{4.17a}$$

Thus, when sL is large the adjustment time to steady state is small compared with the diffusion time L^2/κ just as in the linearized problems discussed e.g. by Veronis (1967*a*, *b*). Needless to say this property is exceedingly valuable in experimental work with stratified fluids.

In terms of the non-dimensional parameter δ_N, (4.17*a*) becomes

$$\delta_N \sim E_N \max(1, sL). \tag{4.17b}$$

Note that (4.17*b*) is consistent with the previous assumption that $\delta_N \ll 1$.

5. First example: region with smooth cross-section

Let us apply (4.14) to the following region (see figure 2)

$$x^2 + z^2 \leqslant R^2, \tag{5.1a}$$

$$0 \leqslant y \leqslant L_y. \tag{5.1b}$$

θ, defined as in §4, is the angle between a normal to the boundary and a horizontal plane. If z is the height at which this normal intersects the boundary we have in this case a unique relation between θ and z given by

$$z = R\sin\theta, \tag{5.2a}$$

where

$$-\tfrac{1}{2}\pi \leqslant \theta \leqslant \tfrac{1}{2}\pi. \tag{5.2b}$$

The parameters $\hat{\rho}$ and s in the boundary condition are chosen as (see figure 2)

$$\left.\begin{aligned} \hat{\rho} &= -Q\sin(\theta + \alpha\,\mathrm{sgn}\,x) && (5.3a)\\ s &= s_0 = \text{constant} && (5.3b)\end{aligned}\right\} \quad \text{on} \quad x^2+z^2 = R^2,$$

$$\left.\begin{aligned} &\hat{\rho}\ \text{not specified} && (5.3c)\\ &s = 0. && (5.3d)\end{aligned}\right\} \quad \text{on} \quad y = (0, L_y).$$

This example is chosen because it illustrates well the behaviour of (4.14) when applied to regions with smooth shape.

Introducing (5.3) into (4.14*c*) we obtain

$$B(z) = \frac{2\kappa L_y s_0}{A\cos\theta}, \quad C(z) = \frac{-2\kappa L_y s_0}{A\cos\theta} Q\sin\theta\cos\alpha. \tag{5.4a}$$

Furthermore, A and dA/dz may be written

$$A = 2L_y R\cos\theta, \quad dA/dz = -2L_y\tan\theta. \tag{5.4b}$$

Introducing (5.4) into (4.14) we obtain

$$\frac{\partial \rho^I}{\partial t} - \kappa \frac{\partial^2 \rho^I}{\partial z^2} + \frac{\kappa \sin\theta}{R\cos^2\theta}\frac{\partial \rho^I}{\partial z} + \frac{\kappa s_0 \rho^I}{R\cos^2\theta} = -Q\frac{\kappa s_0 \sin\theta\cos\alpha}{R\cos^2\theta}. \tag{5.5}$$

This equation is singular at the end-points $z = \pm R$ ($\theta = \pm \frac{1}{2}\pi$). In such cases (e.g. Petrovsky 1954, p. 163) the appropriate boundary condition is generally a

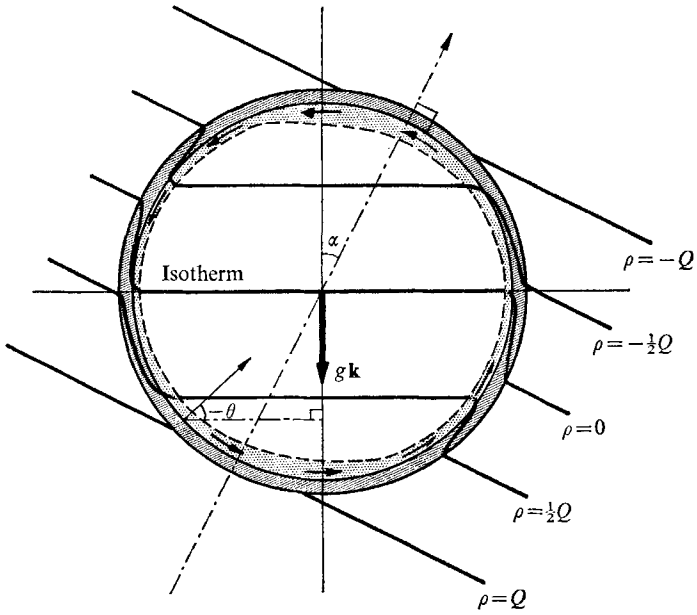

FIGURE 2. Illustrations of isotherms and boundary-layer flow obtained in the example treated in §5. The temperature outside the cylinder is prescribed and increases with constant rate in a direction perpendicular to the cylinder axis and making an angle α with the vertical. The temperature in the main body of the fluid increases in a vertical direction with a rate given by (5.10). This temperature gradient approaches the outside *vertical* gradient when the wall thickness decreases. The illustrated solution is acceptable only if it is gravitationally stable; in this case if $Q > 0$, $0 \leqslant \alpha < \frac{1}{2}\pi$.

regularity condition. Since we expect a physical solution to have finite heat flux and flux convergence, we must require at least

$$\partial \rho^I / \partial z \text{ finite}. \tag{5.6}$$

Then, close to $z = \pm R$ the most differentiated terms (in both space and time) disappear, and (5.5) degenerates to

$$\sin\theta\, \partial \rho^I/\partial z + s_0 \rho^I = -s_0 Q \sin\theta\cos\alpha. \tag{5.7}$$

Let us express (5.6) in terms of θ. Since

$$\partial \rho^I/\partial\theta = R\cos\theta\, \partial\rho^I/\partial z,$$

we obtain from (5.6) the homogeneous boundary condition

$$\partial \rho^I/\partial\theta = 0 \quad \text{at} \quad \theta = \pm\tfrac{1}{2}\pi. \tag{5.8}$$

Equation (5.5) becomes in terms of θ

$$\frac{\partial \rho^I}{\partial t} - \frac{\kappa}{R^2 \cos^2\theta}\left(\frac{\partial^2 \rho^I}{\partial \theta^2} - Rs_0 \rho^I - QRs_0 \sin\theta \cos\alpha\right) = 0. \tag{5.9}$$

A steady solution satisfying (5.8) and (5.9) is immediately found as

$$\rho^I = -Q\frac{Rs_0}{1+Rs_0}\cos\alpha \sin\theta = -Q\frac{Rs_0}{1+Rs_0}\frac{z}{R}\cos\alpha. \tag{5.10}$$

Furthermore, we always have $Rs_0 > 0$ since the thermal conductivity of the wall is positive, which means that the homogeneous steady-state problem has no solution different from zero. Consequently (5.10) represents a unique steady solution.

The boundary-layer transport m for unit length of the cylinder (defined as positive upwards) is obtained from (4.9) and becomes

$$m = \kappa \operatorname{sgn} x(1+Rs_0)\tan\alpha. \tag{5.11}$$

For this particular choice of boundary conditions the transport carried around the container by the boundary layer is constant and the interior is motionless in the steady state. This is so irrespective of whether $Rs_0 \gg 1$ or not, since in this particular case the interior diffusive term, $\kappa(\partial^2\rho^I/\partial z^2)$ in (4.1 *c*), happens to be zero. Equation (5.10) is illustrated schematically in figure 2, for the case $\alpha = 30°$ and $Rs_0 \gg 1$.

5.1. *The singular points* $z = \pm R$

We now have to discuss the behaviour of our system in the vicinity of the singular points $z = \pm R$. From (3.17), we find that the boundary-layer theory breaks down at these points, formally giving rise to infinite boundary-layer thickness. The breakdown may also be described in the following way. A finite distance from the singular point the primary object of the boundary layer is to 'help' the interior density field to satisfy the thermal boundary condition. When approaching a singular point, the boundary layer loses the ability to do this, since $\rho^B \to 0$ unless at the same time $m \to \infty$, which is not physically acceptable. Accordingly, the interior density distribution has to satisfy the boundary condition by itself at these points. The degenerate form (5.7) that the ρ^I equation takes when approaching $z = \pm R$ is identical to the boundary condition at these points. Accordingly, a solution to (5.5), (time dependent or steady) automatically satisfies the thermal boundary condition at $z = \pm R$. This behaviour suggests that the singularities play a passive role only.

The boundary layer does not disappear completely at the singularity, since a finite boundary-layer transport has to be carried across the singular point. The important question is whether the solution in the rest of the container depends on the behaviour of the boundary layer in the vicinity of the singular point. We could derive the equations governing the somewhat thicker boundary layer that appears in the vicinity of $z = \pm R$ (specifically, $\cos\theta \lesssim E_N^{\frac{1}{4}}$; the thickness is $E^{\frac{3}{4}}L$), essentially as in Stewartson (1966). Like Stewartson we shall not attempt an explicit solution since these equations cannot be integrated locally in the same way as the buoyancy-layer equations. An order-of-magnitude analysis shows that

the additional density anomaly required to overcome viscosity and drive the boundary-layer transport across the singular point is small enough to be negligible when introduced in the boundary condition, so that the interaction with ρ^I may be neglected. The dynamics is similar to the case with a finite horizontal surface treated in the next section. Whenever the container has a curved top and bottom equation (4.14) degenerates to the thermal boundary condition in the vicinity of the singular points, and so the same reasoning may be applied to all such containers.

5.2. *Assumption of stable stratification*

Weinbaum (1964) treated a problem formally very similar in appearance to the one we have analyzed in this section. He, however, assumes that there is a large-scale vortex in the interior, which rules out the possibility of a stable stratification. Since in the present paper we make the opposite assumption one might expect contradictory results. This is not the case, however, since we cover different ranges of boundary conditions. Thus, when the present analysis predicts an unstable density distribution (e.g. when $\frac{1}{2}\pi < \alpha \leqslant \pi$, $Q > 0$) the solution has to be rejected (see § 8). In such cases an approach similar to Weinbaum's, assuming an essentially homogeneous interior is probably correct. The question whether in similar situations the appropriate solution contains a stratified core or an essentially homogeneous vortex has been discussed in a recent paper by Brooks & Ostrach (1970).

6. Second example: region with rectangular cross-section

6.1. *Statement of problem*

Next we shall apply equation (4.14) to the region (see figures 3 and 4)

$$0 \leqslant x \leqslant L, \tag{6.1a}$$

$$0 \leqslant y \leqslant L, \tag{6.1b}$$

$$0 \leqslant z \leqslant H. \tag{6.1c}$$

The parameters s and $\hat{\rho}$ in the boundary condition are given by

$$(s, \hat{\rho}) = \begin{Bmatrix} (s_1, \hat{\rho}_1) & \text{at} & x = 0 \\ (s_2, \hat{\rho}_2) & \text{at} & x = L \\ (s_3, \hat{\rho}_3) & \text{at} & y = 0 \\ (s_4, \hat{\rho}_4) & \text{at} & y = L \\ (s_B, \hat{\rho}_B) & \text{at} & z = 0 \\ (s_T, \hat{\rho}_T) & \text{at} & z = H \end{Bmatrix}, \tag{6.2}$$

where s_B, $\hat{\rho}_B$, s_T, $\hat{\rho}_T$, are constants and $s_n, \hat{\rho}_n$ $(n = 1, \ldots, 4)$ are restricted for convenience to be functions of z only. This may be realized, for example, with vertical walls of varying thickness as illustrated in figure 4. Then from (4.14c)

$$B(z) = \frac{\kappa}{L}\sum_1^4 s_n, \quad C(z) = \frac{\kappa}{L}\sum_1^4 s_n \hat{\rho}_n,$$

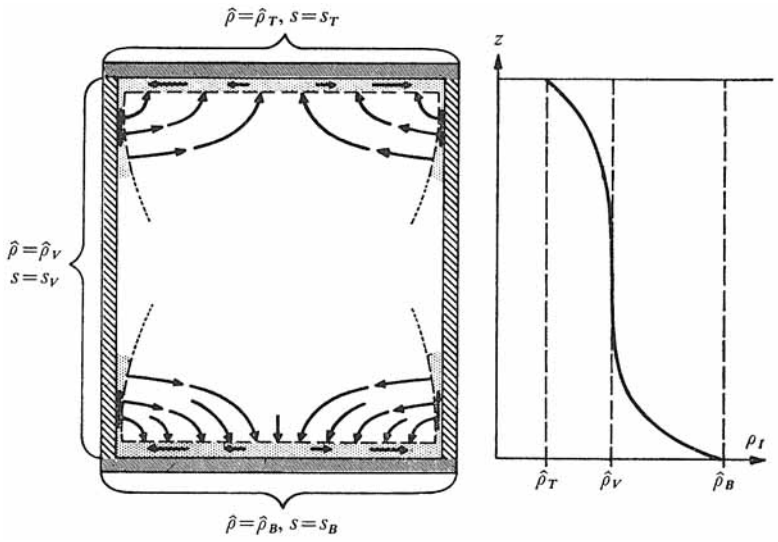

FIGURE 3. The temperature and flow field between two horizontal conducting plates held at different temperatures. The outside of the vertical boundaries are held at an intermediate (environmental) temperature. In order to obtain a linear variation of temperature in the fluid, the vertical boundaries have to be extremely well insulated (6.20).

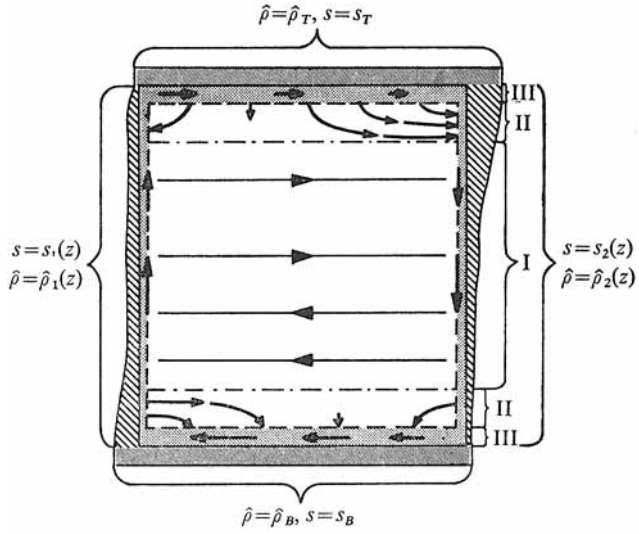

FIGURE 4. Illustration of the different regions obtained when the thermal contact through the vertical boundaries is good in the sense expressed by (6.22). In region I heat diffusion has no influence on the temperature field which is determined for each level individually by the constraint that the total boundary-layer flow through each horizontal plane must vanish. Region II serves to match the temperature field in region I to the boundary condition on the horizontal plates while in region III, the circulation induced in region II and in the vertical boundary layers are tied together.

and equation (4.14b) becomes

$$\frac{\partial \rho^I}{\partial t} - \kappa \frac{\partial^2 \rho^I}{\partial z^2} + \frac{\kappa}{L} \rho^I \sum_1^4 s_n = \frac{\kappa}{L} \sum_1^4 s_n \hat{\rho}_n. \tag{6.3}$$

Equation (6.3) is regular in the whole interval and boundary conditions on ρ^I have to be specified at $z = (0, H)$.

First we discuss these boundary conditions, and then illustrate with two specific cases of (6.2) which have particular relevance to laboratory experiments.

6.2. *The horizontal $E_N^{\frac{1}{4}}$ boundary layer, and the conditions under which their influence is negligible*

The boundary conditions on the complete solution $\rho^I + \rho^B$ are given by

$$\left(\frac{\partial \rho^I}{\partial z} + \frac{\partial \rho^B}{\partial z}\right) = s_B(\rho^I + \rho^B - \hat{\rho}_B) \quad \text{at} \quad z = 0, \tag{6.4a}$$

$$-\left(\frac{\partial \rho^I}{\partial z} + \frac{\partial \rho^B}{\partial z}\right) = s_T(\rho^I + \rho^B - \hat{\rho}_T) \quad \text{at} \quad z = H. \tag{6.4b}$$

Since the theory for the buoyancy layer breaks down when the boundary is horizontal, we are forced to make a special analysis in order to eliminate ρ^B from (6.4). As pointed out by Veronis (1967a), the horizontal boundary layers are analogous to the Stewartson $E^{\frac{1}{3}}$ layer occurring in homogeneous rotating fluids. (There may also be thicker layers analogous to the Stewartson $E^{\frac{1}{4}}$ layer but any such layers are already included in (4.14) and so need no separate discussion.) The governing boundary-layer equations may be found as in § 3. In this case, however, the heat equation may not be linearized in the same way as on non-horizontal boundaries since the leading term in $\mathbf{v} \cdot \nabla \rho^I$ (i.e. $u^B \partial \rho^I / \partial \xi$) is identically zero.

Implicit in (6.2) there is an important assumption, namely that the boundary condition on each horizontal boundary is independent of position. This condition makes it possible though not necessary for ρ^I to satisfy (6.4) without assistance from ρ^B. Furthermore, since in this case the horizontal boundary layer is forced only by the flux coming from the buoyancy layers and not by the boundary condition, we have no reason to restrict the values of s_B and s_T in (6.4). Thus we do not exclude perfectly conducting horizontal boundaries. If the boundary condition were allowed to vary along the horizontal boundaries, ρ^B would be important in (6.4), and thus the boundary condition to be applied on ρ^I would in general be unknown without a complete analysis of the boundary layer.

We shall now try to find out when ρ^B may, however, simply be ignored in (6.4). If

$$\delta_N \ll E_N^{\frac{1}{4}}, \quad sL \ll E_N^{-\frac{1}{3}}, \tag{6.5}$$

we obtain the following (dimensional) boundary-layer equations

$$0 = -\frac{\partial p^B}{\partial x} + \nu \rho_m \frac{\partial^2 U^B}{\partial z^2}, \tag{6.6a}$$

$$0 = -\frac{\partial p}{\partial y} + \nu \rho_m \frac{\partial^2 V^B}{\partial z^2}, \tag{6.6b}$$

$$0 = -\frac{\partial p^B}{\partial z} - \rho^B g, \tag{6.6c}$$

$$\nabla . \mathbf{v}^B = 0, \tag{6.6d}$$

$$W^B \frac{\partial \rho^I}{\partial z} = \kappa \frac{\partial^2 \rho^B}{\partial z^2}. \tag{6.6e}$$

For consistency it is required that

$$\rho^B \sim \frac{m}{\kappa} \epsilon_H^2 \rho^I, \tag{6.7a}$$

$$\epsilon_H \sim E_N^{\frac{1}{3}}, \tag{6.7b}$$

where $\epsilon_H L$ is the boundary-layer thickness, and $m \sim \epsilon_H L U^B$ is the flux in the boundary layer.

A scaling analysis based on (6.6) is valid if the neglected contributions are at most comparable to the terms retained in (6.6). This means that (6.7) remain valid within the much weaker conditions

$$\delta_N \lesssim E_N^{\frac{1}{3}}, \quad sL \lesssim E_N^{-\frac{1}{3}}. \tag{6.8}$$

The horizontal boundary-layer flux has to match with the flux in the buoyancy layer and thus we obtain from (4.9)

$$m \sim s_V L \kappa, \tag{6.9}$$

where $$s_V \sim \max s_n \quad (n = 1, \ldots, 4).$$

(If the sidewalls were not vertical (6.9) would be $m \sim \kappa \max (s_V L, 1)$.)

In order that ρ^B be negligible in (6.4) we must have

$$\rho^B \ll \rho^I \quad \text{when} \quad s_H L \gtrsim \epsilon_H^{-1}, \tag{6.10a}$$

or $$\epsilon_H^{-1} \rho^B \ll s_H L \rho^I \quad \text{when} \quad \epsilon_H^{-1} \gtrsim s_H L \gtrsim 1, \tag{6.10b}$$

or $$\epsilon_H^{-1} \rho^B \ll \rho^I \quad \text{when} \quad 1 \gtrsim s_H L, \tag{6.10c}$$

where $s_H \sim (s_B, s_T)$.

Comparing (6.10) with the previous estimate of ρ^B as deduced from (6.7) and (6.9) we find that (6.10) is satisfied under (6.8) as long as $s_H \gtrsim s_V$, i.e. when the top and the bottom conduct at least as well as the sidewalls. When $s_H \ll s_V$, however, we must require the stronger condition (6.5) to be valid.

We shall not carry the analysis of (6.6) any further, but accept that when (6.8), or (6.5) when $s_H \ll s_V$, is violated, we do not know the proper boundary condition for ρ^I at $z = (0, H)$. Under such conditions, not only is (6.10) not true, but the boundary-layer equations are necessarily non-linear.

The consequences of this lack of knowledge are not, however, too serious, since, as will appear below, ρ^I is unaffected by the boundary condition at $z = (0, H)$, in the main part of the region (i.e. region I as illustrated in figure 4), when $s_V L$ is large. From now on the boundary condition on ρ^I will be taken as

$$\frac{\partial \rho^I}{\partial z} = s_B (\rho^I - \hat{\rho}_B) \quad \text{at} \quad z = 0, \tag{6.11a}$$

$$-\frac{\partial \rho^I}{\partial z} = s_T (\rho^I - \hat{\rho}_T) \quad \text{at} \quad z = H. \tag{6.11b}$$

assuming *either* (6.8) with $s_H \gtrsim s_V$, *or* (6.5), *or* $s_V L \gg 1$ with attention confined to region I of figure 4.

6.3. *Stratification due to an applied vertical temperature contrast*

The classical way to produce a stratified fluid system is to apply different temperature to the top and bottom of a container and consider all other boundaries thermally insulated. We can now treat this case in a realistic way, allowing all boundaries to have finite conductivity, and thereby conclude how well the 'sidewalls' must be insulated for the classical approach to be useful. We shall find ((6.20) below) that it is necessary among other things that *the thermal thickness* $d^* \equiv Kd/\hat{K}$ *of the sidewalls is much larger than the overall dimensions of the fluid region*; *see table* 1.

Let us consider the following special case of (6.2) (illustrated in figure 3)

$$(s_n, \hat{\rho}_n) = (s_V, \hat{\rho}_V), \quad (n = 1, \ldots, 4), \tag{6.12}$$

where s_V and $\hat{\rho}_V$ are constant. In this case (6.3) becomes

$$\frac{\partial \rho^I}{\partial t} - \kappa \frac{\partial^2 \rho^I}{\partial z^2} + \frac{\kappa}{L} 4 s_V \rho^I = \frac{\kappa}{L} 4 s_V \hat{\rho}_V. \tag{6.13}$$

Equation (6.13) subject to the boundary conditions (6.11) has the following *steady* solution

$$\rho^I = \hat{\rho}_V + C_1 \exp(-\alpha z) + C_2 \exp \alpha(z - H), \tag{6.14}$$

where

$$\alpha = 2(s_0/L)^{\frac{1}{2}}, \tag{6.15a}$$

$$C_1 = \frac{s_B(s_T + \alpha)(\hat{\rho}_B - \hat{\rho}_V) - s_T(s_B - \alpha)(\hat{\rho}_T - \hat{\rho}_V)\exp(-\alpha H)}{(s_B + \alpha)(s_T + \alpha) - (s_B - \alpha)(s_T - \alpha)\exp(-2\alpha H)}, \tag{6.15b}$$

and C_2 is obtained from the expression for C_1 by simply exchanging the indices B and T. If

$$\alpha \ll s_H, \tag{6.16}$$

equation (6.15b) is approximated by

$$C_1 = \frac{(\hat{\rho}_B - \hat{\rho}_V) - (\hat{\rho}_T - \hat{\rho}_V)\exp(-\alpha H)}{1 - \exp(-2\alpha H)}, \tag{6.17}$$

which is the form obtained from the boundary conditions $\rho^I = \hat{\rho}_B$ at $z = 0$ and $\rho^I = \hat{\rho}_T$ at $z = H$. Consequently (6.16) is the condition that allows the top and bottom boundaries to be considered good conductors.

Introduction of (6.17) into (6.14) and expansion for small αH yields

$$\rho^I = \hat{\rho}_B + (\hat{\rho}_T - \hat{\rho}_B)\frac{z}{H} + O(\alpha H). \tag{6.18}$$

Thus if

$$\alpha H \ll 1, \tag{6.19}$$

the solution degenerates to the ideal solution corresponding to insulated sidewalls and conducting top and bottom, Consequently (6.16) and (6.19) are the necessary conditions for producing a linear stratification with a 'conventional' experimental set up. The experimental difficulty is connected primarily with (6.19). Making use of (3.10) and (6.15a) we may write (6.19) as

$$d^* = dK/\hat{K} \geqslant 4H^2/L. \tag{6.20}$$

In the opposite (more realistic) case when $\alpha H \gg 1$ the solution (6.14) degenerates to $\rho^I = \hat{\rho}_V$ everywhere except in regions of boundary-layer character close to $z = (0, H)$.

If, simultaneously, $$\alpha \ll s_H, \quad \alpha H \gg 1, \tag{6.21a}$$

the steady solution simplifies to

$$\rho^I = \hat{\rho}_V + (\hat{\rho}_B - \hat{\rho}_V)\exp(-\alpha z) + (\hat{\rho}_T - \hat{\rho}_V)\exp\alpha(z-H). \tag{6.21b}$$

The density field and the associated circulation in this case are illustrated in figure 3. The vanishing of $\partial\rho^I/\partial z$ in part of the interior means of course that our scale analysis breaks down. This, however, does not invalidate the prediction for $\rho^I(z)$, since where $\partial\rho^I/\partial z$ vanishes the strength of the buoyancy layer vanishes as well.

6.4. *General results for second example, when* $1 \ll s_V L \ll E_N^{-\frac{1}{2}}$

Let us now discuss the system defined by (6.3) and (6.11) in more generality. Since (6.3) contains non-constant coefficients, we cannot solve the most general case explicitly. However, under the restriction

$$s_V L \gg 1, \tag{6.22}$$

the steady solution may be approximated by

$$\rho^I = \rho_0^I + \rho_T^I + \rho_B^I, \tag{6.23a}$$

where only the first term is significant throughout most of the interior, and is

$$\rho_0^I = \sum_1^4 s_n \hat{\rho}_n \Big/ \sum_1^4 s_n. \tag{6.23b}$$

Formally (ρ_B^I, ρ_T^I) satisfy the following equations

$$-\frac{\partial^2}{\partial z^2}\rho_B^I + L^{-1}\left(\sum_1^4 s_n\right)_{z=0}\rho_B^I = 0, \tag{6.23c}$$

$$-\frac{\partial^2}{\partial z^2}\rho_T^I + L^{-1}\left(\sum_1^4 s_n\right)_{z=H}\rho_T^I = 0, \tag{6.23d}$$

subject to the boundary conditions

$$\frac{\partial}{\partial z}\rho_B^I = s_B(\rho_0^I + \rho_B^I - \hat{\rho}_B) \quad \text{at} \quad z = 0, \tag{6.23e}$$

$$-\frac{\partial}{\partial z}\rho_T^I = s_T(\rho_0^I + \rho_T^I - \hat{\rho}_T) \quad \text{at} \quad z = H, \tag{6.23f}$$

$$\rho_B^I \to 0 \quad \text{when} \quad z \to \infty, \tag{6.23g}$$

$$\rho_T^I \to 0 \quad \text{when} \quad H - z \to \infty. \tag{6.23h}$$

Equations (6.23) represents a boundary-layer approach to the interior problem. This 'interior boundary layer' corresponds to the $E_N^{\frac{1}{4}}$ layer found by Veronis (1967*a*), but because of our basic assumption $s_V L \ll E_N^{-\frac{1}{2}}$, the thickness is here independent of E_N.

The boundary-layer approximations we must make to obtain (6.23) are: (i) The heat diffusion connected with ρ_0^I, i.e. the contribution $-\kappa\partial^2\rho_0^I/\partial z^2$ to the second term in (6.3), is neglected. (ii) The variable coefficient $\left(\sum_1^4 s_n\right)$ is replaced by its value on the upper (lower) boundary when multiplying $\rho_T^I(\rho_B^I)$ in (6.3). (iii) ρ_T^I is neglected in the lower and ρ_B^I in the upper boundary condition. (iv) $\partial\rho_0^I/\partial z$ is neglected in the boundary conditions. (However, we retain $\partial\rho_B^I/\partial z$ and $\partial\rho_T^I/\partial z$ to allow formally for possibilities such as $s_B \lesssim (s_V/L)^{\frac{1}{2}}$.)

These approximations are justified when ρ_0^I varies only on the length scale L, and (ρ_T^I, ρ_B^I) decays on a length scale short compared with L when leaving the upper and lower boundaries. From (6.23*c* and *d*) we find that this is true when (6.22) is satisfied.

(ρ_T^I, ρ_B^I) may be obtained from (6.23) by elementary methods. For illustrative purposes we will here write down the solution in the case where s_B and s_T are sufficiently large for the top and bottom boundaries to be considered good conductors. We obtain

$$\rho_B^I = (\hat{\rho}_B - \rho_0^I(z=0))\exp(-\alpha_B z), \tag{6.24a}$$

$$\rho_T^I = (\hat{\rho}_T - \rho_0^I(z=H))\exp -\alpha_T(H-z), \tag{6.24b}$$

where

$$\alpha_B^2 = L^{-1}\left(\sum_1^4 s_n\right)_{z=0}, \tag{6.24c}$$

$$\alpha_T^2 = L^{-1}\left(\sum_1^4 s_n\right)_{z=H}. \tag{6.24d}$$

When treating the time-dependent behaviour of ρ^I we may split the solution in a way similar to (6.23*a*). For the interior part ρ_0^I, we obtain immediately

$$\frac{\partial}{\partial t}\rho_0^I(z,t) = -\frac{\kappa}{L}(\rho_0^I(z,t) - \rho_0^I(z,t=\infty))\sum_1^4 s_n, \tag{6.25}$$

where $\rho_0^I(z, t=\infty)$ is identical to the steady solution given by (6.23*b*).

6.5. *Further discussion of the case* $1 \ll s_V L \ll E_N^{-\frac{1}{2}}$

Let us now recapitulate the physical picture we have found in the case $s_V L \gg 1$. The system may be divided into three regions according to figure 4. In I, the density field is determined by equation (6.23*b*). In this region the diffusion-associated vertical velocity in the interior gives rise to a negligible contribution to the vertical volume transport, and consequently the net boundary-layer transport (M^B) has to vanish in a steady state. This means that ρ^I adopts the value which makes this possible for each level individually.

The thickness of region II is of order $(L/s_V)^{\frac{1}{2}}$, which is precisely small enough for vertical diffusion to balance the vertical advection of an interior flux whose order of magnitude equals that of the flux carried by the buoyancy layer. If we decrease the thickness of the vertical boundaries and thus increase s_V the buoyancy-layer flux increases and consequently the thickness of region II decreases. Furthermore, in region II, the interior density distribution adjusts to the boundary condition at the top and bottom, which is possible because vertical diffusion can effect the density field in this region.

Finally, we have region III, which contains the degenerate horizontal boundary layer. This region supports the flux carried to the corners by the buoyancy layers, communicates flow from one corner to another, and distributes evenly the net flux supplied by the buoyancy layer over the horizontal cross-section before feeding it back into region II.

For the same physical reasons, nested diffusive regions like II and III can also occur at interior levels z where ρ_0^I as given by (6.23*b*) has a discontinuity. If ρ_0^I is continuous but contains discontinuous individual terms, only a region like III will occur at the corresponding level.

7. A laboratory experiment

A simple experiment has been carried out in order to test the qualitative results illustrated in figure 4. The experimental fluid was confined between two constant-temperature baths. The thickness of the wall facing the cold bath increased linearly with height while the thickness of the opposite wall, facing the hot bath decreased with height. The mean thickness of these vertical boundaries, which were made of Plexiglass, was chosen sufficiently small for (6.22) to be valid, and consequently region I was expected to fill the major part of the fluid system. The observations demonstrated the existence of a stably stratified almost stagnant interior enclosed by laminar boundary layers. Furthermore, the time required for the interior temperature distribution to come to equilibrium was much shorter than the purely diffusive scale, as predicted by (4.17) when $sL \gg 1$.

The vertical distribution of temperature was measured with a thermistor arrangement. With the cold bath at 20 °C and the hot at 40 °C, the fluid temperature varied from about 24 °C at the bottom to about 31 °C at the top of the region. No horizontal temperature variation could be detected outside the buoyancy layers. Since the boundary condition particularly at the walls facing the surrounding air was not accurately known, a quantitative comparison with (6.23*b*) is not appropriate, but the qualitative agreement seems reasonable. The fluid motion was visualized by means of the technique described by Baker (1966) (see figure 5, plate 1).

In this experiment the upper boundary was simply a free surface facing the surrounding air. Consequently the fluid was slightly cooled from above which means that the temperature gradient had to change signs, or at least tend to zero, somewhere close to the top of the system. This means that our description breaks down at least locally (for example the boundary-layer transport formally tends to infinity when $\partial\rho^I/\partial z = 0$ according to (4.9)). The observations also showed a somewhat irregular behaviour in the uppermost part of the fluid region. However, this irregularity did not seem to influence the behaviour of the major part of the system (i.e. region I in figure 4). This provides additional support for the idea that, when $s_T L \ll 1$, the upper and lower boundary conditions need not be of crucial importance, if the stably stratified interior is the region of interest in a particular experiment.

8. Concluding remarks

The analysis of §§2–4 reduces the problem of finding the interior density field $\rho^I(z,t)$ to solving (4.14). For containers with flat horizontal portions the corresponding boundary layer often need not be considered in detail. Sufficient conditions for this, in the case of thermally uniform flat portions, are summarized at the end of §6.2 and illustrated via the experimentally important cases of §§6.3 and 6.4.

8.1. *Summary of conditions for validity of the general theory of* §§2–4

Among the basic restrictions we have imposed on our fluid system are the postulate (2.4) that temperature differences in the interior should be comparable with those imposed exterior to the finitely conducting boundary, i.e.

$$\rho^I \sim \hat{\rho}. \tag{8.1a}$$

To this condition we now add another qualitative condition on ρ^I, namely

$$\partial\rho^I/\partial z < 0, \tag{8.1b}$$

which follows from the requirement that the solution has to be gravitationally stable, if the prediction is to be physically meaningful. We cannot expect (8.1*b*) to appear from the analysis; gravitational instability is ruled out when we assume hydrostatic balance in the interior (2.8).

The basic restrictions on the parameters of the system are given by (2.7) and (3.9). These can be conveniently restated using relations (3.13*a*) and (3.14) found during the analysis. We obtain

$$E_N \ll 1, \tag{8.2a}$$

$$sL \ll E_N^{-\frac{1}{2}}, \tag{8.2b}$$

$$\delta_N \ll 1, \tag{8.2c}$$

$$\sigma \sim 1, \tag{8.2d}$$

where it will be recalled that $E_N = \nu/NL^2$, $\delta_N = (\tau N)^{-1}$ (N is the buoyancy frequency and τ the timescale), s is the conductance parameter in the thermal boundary condition $\mathbf{n}.\nabla\rho = s(\rho - \hat{\rho})$, L is a scale for the size of the container, and σ is the Prandtl number.

Equation (8.2*a*) gives rise to the boundary-layer character of the fluid system, in that it limits the strength of diffusion of momentum and heat.

Equation (8.2*b*) limits the heat flux through the boundary of the region, which means limiting the strength with which the fluid system is driven. Equation (8.2*b*) originally appeared from the need to linearize the heat balance in the buoyancy layer. The relation (3.14) between sL and R_N subsequently obtained shows however that (8.2*b*) is also a sufficient condition for our original restriction on R_N (2.7) to be fulfilled, ensuring hydrostatic balance in the interior, and linear momentum balance in the boundary layer.

Equation (8.2*c*) requires that the characteristic forcing frequency should be much smaller than the buoyancy frequency. Equation (8.2*d*), finally, has been adopted essentially for convenience. The analysis can easily be generalized to many cases involving large or small σ.

We have also imposed a geometrical condition (§2, before (2.9a)) namely that each horizontal cross-section of the region should be a connected surface. (An extension to more general shapes would in general involve detached horizontal shear layers; compare §6.5). In summary, this geometrical condition together with (8.1) and (8.2) is sufficient for formal validity of the analysis of §§2–4. While (8.2) is expressed in terms of quantities known *a priori*, (8.1) must be checked *a posteriori* when a particular solution has been obtained.

8.2. *Implications for laboratory experiments*

Equations (4.15), (6.23b) and (6.25) describing the density field in the main part of the region, are powerful tools for experimental work since the interior density distribution may be adjusted to whatever stable distribution is needed. Furthermore, the time required for the steady solution to re-establish itself, when the system has been perturbed, may be controlled simply by choosing a suitable mean thickness of the vertical boundaries. Observe that it is sufficient to allow the boundary thickness to vary with z in order to obtain a prescribed stratification. Consequently it is sufficient for most purposes to have two constant-temperature baths available.

Note also that the method of imposing a vertical temperature difference directly via conducting top and bottom boundaries is comparatively *inconvenient* in the laboratory when $E_N \ll 1$. This is because the adjustment time is the diffusion time, and the requirement on the insulating sidewalls is exceedingly stringent, viz. (6.19).

8.3. *Further discussion of the validity of the basic approximations*

Table 1 indicates that condition (8.2b) (expressed in the form (3.10b)) is sometimes a rather serious restriction, and thus it is of interest to discuss the error we make if this condition is violated. Equation (8.2b) is the basis for two simplifications in the treatment of the boundary layer, namely the linearization of $\mathscr{N}_\rho = \mathbf{v}.\nabla\rho$ in equation (3.2) and the neglect of ρ^B (not $\partial\rho^B/\partial\zeta$) in the thermal boundary condition (3.3b). The first approximation is vital for the success of the analysis, while the latter was adopted merely for reasons of consistency.

The error associated with the linearization of $\mathscr{N}_\rho$, however, is not too serious even when $sL \gtrsim E_N^{-\frac{1}{2}}$. Actually both Gill (1966) and McIntyre (1968) obtained quite good results in the case $sL = \infty$ even though departures from the linearized form of $\mathscr{N}_\rho$ were taken account of only crudely. The reason for this is that even when $sL = \infty$ the linear contribution to $\mathscr{N}_\rho$ is still an important term in the heat balance as long as $\rho^I \gtrsim \rho^B$, ρ^I being the interior density field and ρ^B the boundary-layer contribution to the density field. That is, only when the interior is essentially homogeneous does the 'linear' term $\mathbf{v}^B.\nabla\rho^I$ become unimportant.

The error in the boundary-layer flux created by the linearization of $\mathscr{N}_\rho$ may be estimated by an iterative procedure and becomes approximately

$$\tfrac{1}{4}sL(E_N^{-\frac{1}{2}} + sL)^{-1}\,\hat{Q}/Q,$$

$\hat{Q}$ and Q being the scale of density variation in the boundary condition and the interior respectively. We can see that as long as $\hat{Q}/Q \sim 1$ the error does not exceed 25 % for any value of sL. The most important condition for the linearization to be qualitatively useful is in fact that $\hat{Q}/Q$ is not too large.

The author wishes to thank Professor Bert Bolin, Mr Sven Grahn, Dr Michael E. McIntyre and a referee for the paper for their helpful comments on the manuscript, Miss Inger Albrecktsson for preparing the drawings and Mr Sven Å. Odh for arranging the experiment. This paper is contribution no. 225 from the International Meteorological Institute in Stockholm.

REFERENCES

Baker, D. J. 1966 A technique for the precise measurement of small fluid velocities. *J. Fluid Mech.* **26**, 573.

Barcilon, V. & Pedlosky, J. 1967 On the steady motions produced by a stable stratification in a rapidly rotating fluid. *J. Fluid Mech.* **29**, 673.

Brooks, I. H. & Ostrach, S. 1970 An experimental investigation of natural convection in a horizontal cylinder. *J. Fluid Mech.* **44**, 545.

Gill, A. E. 1966 The boundary-layer régime for convection in a rectangular cavity. *J. Fluid Mech.* **26**, 515.

McIntyre, M. E. 1968 The axisymmetric convective régime for a rigidly bounded rotating annulus. *J. Fluid Mech.* **32**, 625.

Petrovsky, I. G. 1954 *Lectures on Partial Differential Equations.* Cambridge University Press.

Stewartson, K. 1966 On almost rigid rotations. Part 2. *J. Fluid Mech.* **26**, 131.

Veronis, G. 1967*a* Analogous behaviour of homogeneous, rotating fluids and stratified, non-rotating fluids. *Tellus*, **19**, 326.

Veronis, G. 1967*b* Analogous behaviour of rotating and stratified fluids. *Tellus*, **19**, 620.

Weinbaum, S. 1964 Natural convection in a horizontal circular cylinder. *J. Fluid Mech.* **18**, 409.

Yih, C-S. 1965 *Dynamics of Nonhomogeneous Fluids.* Macmillan.

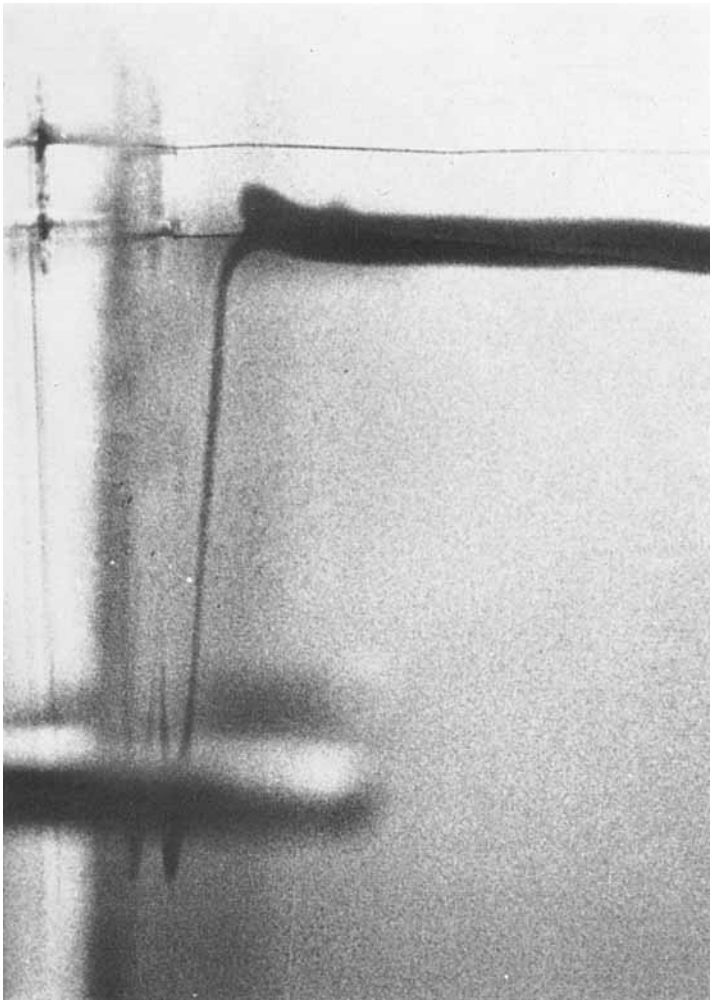

FIGURE 5. Picture of a dye line distorted by the flow in the boundary layer along the cold wall. The picture was taken about 90 sec after the dye line around the lower of the two thin platinum threads were created. The weak counterflow in the outer part of the boundary layer is visible, though an irrelevant distortion of the dye created by the presence of the thread disturbs the picture. The distance between the two threads was close to 5 mm. The mirror image of the dye line, visible in the lower part of the picture, indicates the position of the Plexiglass wall. The threads were situated about halfway between the containers top and bottom.